Electronic Supplementary Material (ESI) for Physical Chemistry Chemical Physics.
This journal is © the Owner Societies 2023

Supporting Information

Pyrogallol functionalized silica nanoparticles and determination of performance parameters in Au (III) adsorption by Taguchi method

Mustafa Can*[a,b], Engin Deniz PARLAR[a], Mustafa AKÇİL[a], Abdülkadir Kızılarslan[c], Semra Boran[d], Abdullah Hulusi Kökçam[d], Özer Uygun[d],

[a]Department of Metallurgical and Materials Engineering, Sakarya University of Applied Sciences, Sakarya, Turkey.

[b]Technologies Application and Research Center (BIYOTAM), Sakarya University of Applied Sciences, Sakarya, Turkey

[c]Engineering Faculty, Department of Metallurgical & Materials Engineering, Sakarya University, Esentepe Campus, 54187 Sakarya, Turkey.

[d] Department of Industrial Engineering, Faculty of Engineering, Sakarya University, Sakarya, Turkey.

* **Corresponding Author:**

Mustafa Can, Sakarya University of Applied Sciences, Technology Faculty, Department of Metallurgical and Materials Engineering, Esentepe Campus, 54187, Sakarya, Turkey. mstfacan@gmail.com; Tel.: +90 (264) 616 05 89

1. Taguchi Experimental Design

Table S1. Taguchi random experiment orders, their levels, and C_e results.

	pH	Agitation rate (rpm)	Adsorbent (gram)	Temperature (°C)	C_0 (mg/L)	Time (minute)	C_e (mg/L)
Experiment 9	3	250	0.4	20	100	30	5.4 4.8
Experiment 10	3	300	0.025	30	150	60	113.4 115.3
Experiment 13	4	200	0.4	30	300	5	0.12 0.18
Experiment 17	5	150	0.4	40	50	60	25.1 25.7
Experiment 21	6	100	0.4	50	150	15	2.4 2.5
Experiment 1	2	100	0.025	20	50	5	16.4 16.8
Experiment 20	5	300	0.1	20	300	15	122.3 122.8
Experiment 8	3	200	0.2	70	50	15	7.9 8.0
Experiment 12	4	150	0.2	20	150	90	19.6 19.3
Experiment 2	2	150	0.050	30	100	15	88.2 91.3
Experiment 15	4	300	0.050	50	50	30	40.9 45.3
Experiment 16	5	100	0.2	30	600	30	501.5 511.5
Experiment 18	5	200	0.025	50	100	90	89.8 91.1
Experiment 14	4	250	0.025	40	600	15	520 505
Experiment 24	6	250	0.1	30	50	90	24.7 24.9
Experiment 6	3	100	0.050	40	300	90	259.3 258.8
Experiment 5	2	300	0.4	70	600	90	479.5 490.0
Experiment 7	3	150	0.1	50	600	5	527.5 528.5
Experiment 11	4	100	0.1	70	100	60	34.5 34.5
Experiment 25	6	300	0.2	40	100	5	98.8 97.9
Experiment 4	2	250	0.2	50	300	60	276.5 277.5
Experiment 23	6	200	0.050	20	600	60	584.0 576.0
Experiment 22	6	150	0.025	70	300	30	264.3 260.3
Experiment 19	5	250	0.050	70	150	5	121.9 136.2
Experiment 3	2	200	0.1	40	150	30	142.6 137.3

Table S2. Taguchi experiments, their levels, capacity results, and S/N ratios.

Exp. No	pH	Speed (rpm)	Mass (gr)	Temp. (°C)	Initial Conc. (mg/L)	Time (min)	q_{e1}	q_{e2}	S/N ratio
1	2	100	0.025	20	50	5	67.20	66.40	36.4951
2	2	150	0.05	30	100	15	11.80	8.70	19.9154
3	2	200	0.1	40	150	30	3.70	6.35	13.1049
4	2	250	0.2	50	300	60	5.88	5.63	15.1948
5	2	300	0.4	70	600	90	15.06	13.75	23.1433
6	3	100	0.05	40	300	90	40.70	41.20	32.2446
7	3	150	0.1	50	600	5	36.25	35,75	31.1254
8	3	200	0.2	70	50	15	10.53	10.50	20.4362
9	3	250	0.4	20	100	30	11.80	11.90	21.4741
10	3	300	0.025	30	150	60	73.20	69.40	37.0525
11	4	100	0.1	70	100	60	32.75	32.80	30.3108
12	4	150	0.2	20	150	90	32.60	32.68	30.2750
13	4	200	0.4	30	300	5	37.49	37.48	31.4772
14	4	250	0.025	40	600	15	160.00	190.00	44.7649
15	4	300	0.05	50	50	30	9.10	4.70	15.4253
16	5	100	0.2	30	600	30	24.63	22.13	27.3396
17	5	150	0.4	40	50	60	3.11	3.04	9.7552
18	5	200	0.025	50	100	90	20.40	17.80	25.5603
19	5	250	0.05	70	150	5	28.10	13.80	24.8695
20	5	300	0.1	20	300	15	88.85	88.60	38.9609
21	6	100	0.4	50	150	15	18.45	18.44	25.3176
22	6	150	0.025	70	300	30	71.40	79.40	37.5107
23	6	200	0.05	20	600	60	16.00	24.00	25.4957
24	6	250	0.1	30	50	90	12.65	12.55	22.0072
25	6	300	0.2	40	100	5	0.30	0.53	-8.6543

2. Speciation of Au (III) in Chloride Media

To simulate the metal ion speciation under optimum conditions calculated with Hydra and Medusa [1] software, and results shown in Figure S1.

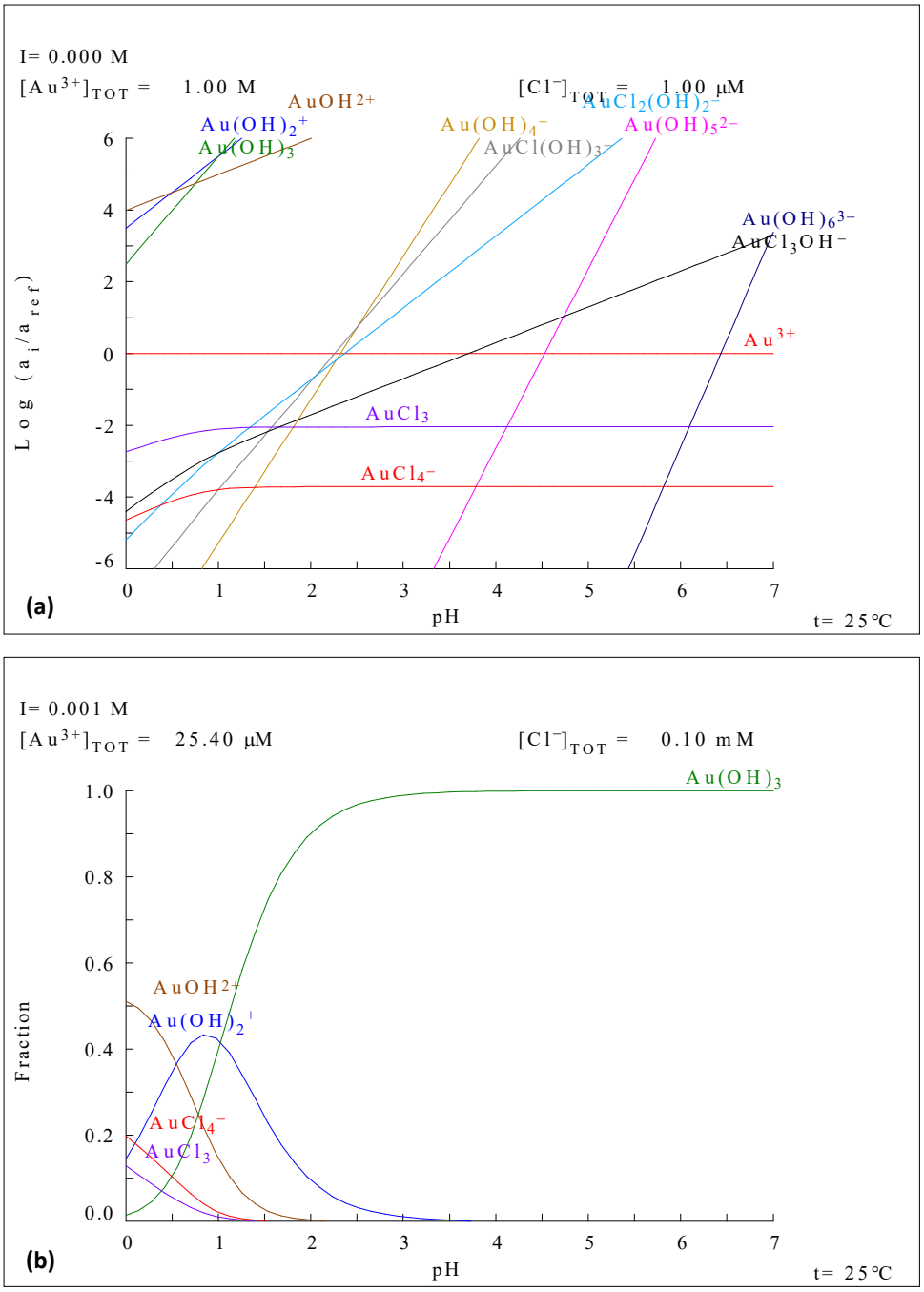

Figure S1. Au (III) relative activities (a) and speciation (b) graphics under 0.0001 M HCl concentrations.

3. Adsorption kinetics

Adsorption kinetics that is examining the change of adsorption on solid surfaces from solutions up to reaching equilibrium, a suitable kinetic model is needed to analyze the rate data. With the development of the adsorption equilibrium theory on heterogeneous solid surfaces, the development of the kinetic adsorption-desorption theory has has also progressed [2]. In order to understand best fitting the kinetic theory and its equation of studied metal ion adsorption kinetics, the pseudo first and pseudo second order, Elovich, and intraparticle diffusion equations were applied. These isotherms, linear forms, and their constants can be seen at **Table S3**.

Table S3. Used adsorption kinetic equations and its linear forms.

	Equation	Linear From	Constants
Lagergren first-order [3]	$\frac{dq_t}{dt} = k_1(q_e - q_t)$	$\log(q_e - q_t) = \log q_e - \frac{k_1}{2{,}303}t$	k_1 (min.$^{-1}$)
Pseudo second-order [4]	$\frac{dq_t}{dt} = k_2(q_e - q_t)^2$	$\frac{t}{q_t} = \frac{1}{kq_e^2} + \frac{1}{q_e}t$	$k_2(g.mg^{-1}.min.^{-1})$
Elovich [5,6]	$\frac{dq_t}{dt} = \propto e^{-\beta q_t}$	$q_t = \frac{1}{\beta}\ln(\propto\beta) + \frac{1}{\beta}\ln t$	$\propto (mg.g^{-1}.min.^{-1})$ $\beta\ (mg.g^{-1})$
Intraparticle diffusion [7]	$q_t = k_{int}t^{1/2}$		$k_{int}\ (mg.g^{-1}.min.^{-\frac{1}{2}})$

An adsorption-desorption kinetics can include the following four steps: external diffusion from solution to interface, diffusion into pores, diffusion of molecules on surface, and realization of adsorption-desorption process [2,8]. Integrated linear pseudo-first and pseudo-second order, Elovich, and intraparticle diffusion kinetic equation form function graphics and their R^2 values can be seen in **Figure S2**.

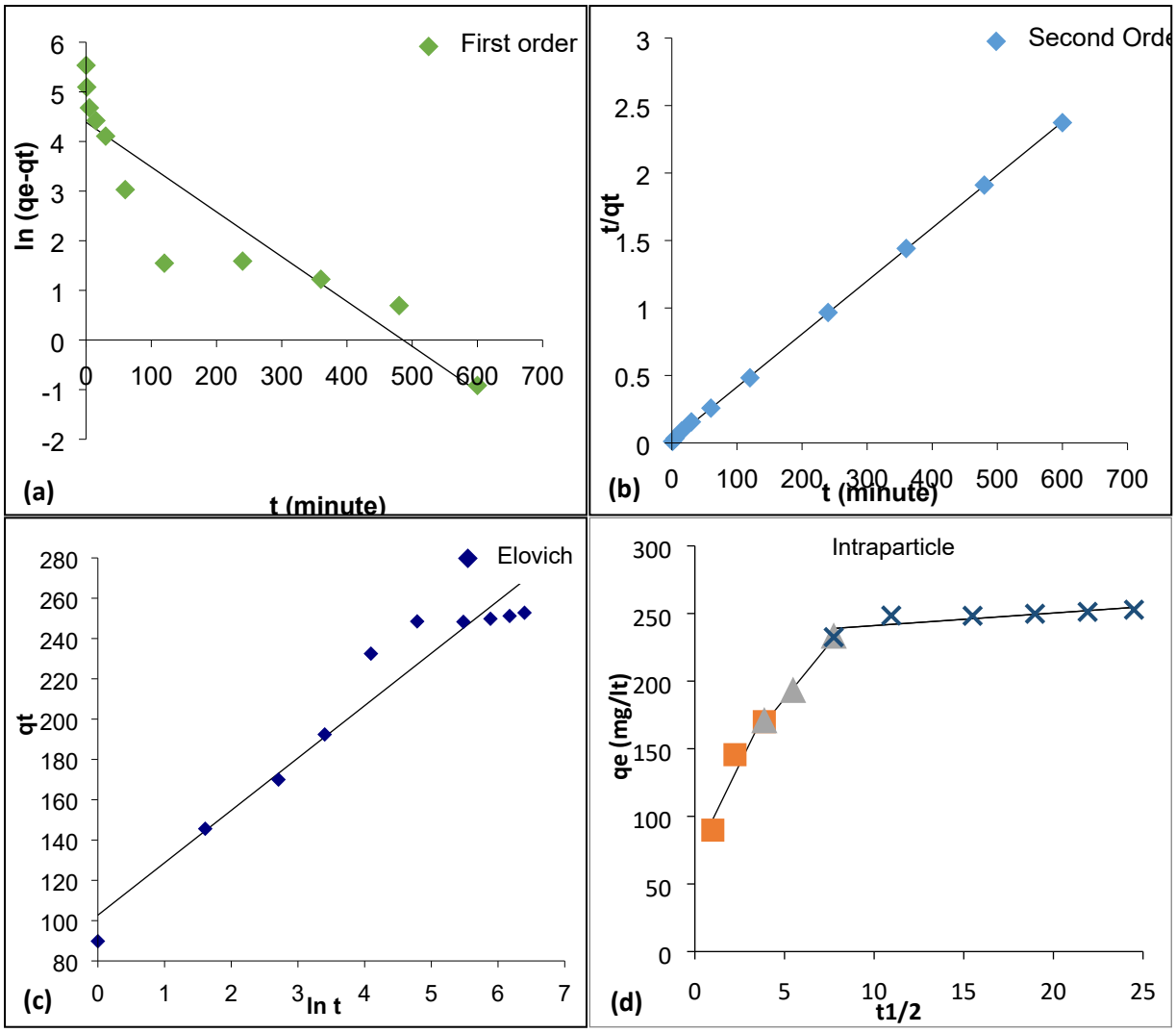

Figure S2. Pseudo-first (a), pseudo-second (b) order, Elovich (c), and intraparticle diffusion (d) kinetic equation parameters and R^2 values for Au (III) adsorption onto APMCM41-Py nanoparticles.

4. Adsorption Isotherms

In order to In order to determine which isotherm equation and its theory fitted the adsorption equilibrium state, Langmuir [9], Modified Langmuir [10], Freundlich [11], Temkin [12], Dubinin–Radushkevich [13,14], and Redlich–Peterson [15] were selected to explicate precious metal ions–TRIS beads interactions. These isotherms and its linear forms can be seen at Table S4.

The Langmuir equation initially derived from kinetic studies has been based on the assumption that on the adsorbent surface there is a definite and energetically equivalent

number of adsorption sites. The bonding to the adsorption sites can be either chemical or physical, but it must be sufficiently strong to prevent displacement of adsorbed molecules along the surface. Thus, localised adsorption was assumed as being distinct from non-localised adsorption, where the adsorbed molecules can move along the surface. Because the bulk phase is constituted by a perfect gas, lateral interactions among the adsorbate molecules were neglected. On the energetically homogeneous surface of the adsorbent a monolayer surface phase is thus formed. Langmuir, for the first time, introduced a clear concept of the monomolecular adsorption on energetically homogeneous surfaces [9,16].

The K_L and K_{ML} are the Langmuir isotherm constants. In this study, unit of K_L is L/mg and K_{ML} is dimensionless constants. Due to the Langmuir equilibrium constant, K_L, is not being dimensionless, it is not theoretically suitable for using in thermodynamic calculations. Instead, the Modified Langmuir isotherm has been proposed and the equilibrium constant is unitless [10]. The theoretical monolayer saturation capacity, q_m, dimension is given as mg/g.

Table S4. Adsorption isotherms and its lineer forms.

	Isotherm	**Linear Form**	**X & Y**	**Slope & cut-off point**
Langmuir [17,18]	$q_e = \frac{q_m K_L C_e}{1 + K_L C_e}$	$\frac{C_e}{q_e} = \frac{1}{q_m K_L} + \frac{C_e}{q_m}$	$x = C_e$ $y = C_e/q_e$	$\tan\alpha = \frac{1}{q_m}$ $cutoff = \frac{1}{K_L q_m}$
Modified Langmuir [10]	$q_e = \frac{q_m K_{ML} C_e}{(C_S - C_e) + K_{ML} C_e}$	$\frac{C_e}{q_e} = \frac{C_s}{q_m K_{ML}} + \frac{(K_{ML} - 1) C_e}{K_{ML} q_m}$		$\tan\alpha = \frac{(K_{ML} - 1)}{K_{ML} q_m}$ $cutoff = \frac{C_s}{q_m K_{ML}}$
Freundlich [11]	$q_e = K_f C_e^{1/n}$	$\log q_e = -\log K_f + \frac{1}{n}\log C_e$	$x = \log c_e$ $y = \log q_e$	$\tan\alpha = \frac{1}{n}$ $cutoff = -\log K_f$
Temkin [12]	$q_e = \frac{RT}{b}\ln(AC_e)$, $RT/b = B$	$q_e = B\ln A + B\ln C_e$	$x = \ln C_e$ $y = q_e$	$\tan\alpha = B$ $cutoff = B\ln A$
(D-R) [13,14]	$q_e = q_m e^{-\beta\varepsilon^2}$	$\ln q_e = \ln q_m - \beta\varepsilon^2$	$x = \varepsilon^2$ $y = \ln q_e$	$\tan\alpha = \beta$ $cutoff = q_m$

	$\varepsilon = RT\left(1 + \frac{1}{C_e}\right)$			
(R-P) [15]	$q_e = \frac{AC_e}{1 + BC_e^g}$	$\ln\left(A\frac{C_e}{q_e} - 1\right) = g\ln\left(C_e\right) + \ln\left(B\right)$	-	-

The essential features of the Langmuir isotherm can be expressed in terms of a dimensionless constant called separation factor (R_L) which is defined by the following equation

$$R_L = \frac{1}{1 + K_L C_o} \quad (1)$$

where C_0 (mg/L) is the initial metal ion concentration and K_L (L/mg) is the Langmuir constant related to the energy of adsorption. In this context, the value of R_L indicates the shape of the isotherms to be either unfavorable ($R_L > 1$), linear ($R_L = 1$), favorable ($0 < R_L < 1$) or irreversible ($R_L = 0$) [19,20].

The Freundlich isotherm is an empirical equation employed to describe heterogeneous systems and equation shown in Table S2. In this equation, K_f, ($mg^{1-1/n}L^{1/n}g^{-1}$) is the Freundlich constant related to the bonding energy, and n, (g/L) is the heterogeneity factor. The slope (1/n) ranges between 0 and 1 is a measure of adsorption intensity or surface heterogeneity, and it becomes more heterogeneous when its value gets closer to zero. Whereas, a value below unity implies chemisorptions process where 1/n above one is an indicative of cooperative adsorption [2,19].

By ignoring the extremely low and large value of concentrations, the derivation of the Temkin isotherm assumes that the fall in the heat of sorption is linear rather than logarithmic. Temkin equation is excellent for predicting the gas phase equilibrium, conversely complex adsorption systems including the liquid-phase adsorption isotherms

are usually not appropriate to be represented [21]. In this equation, A (L/mg) is the equilibrium binding constant corresponding to the maximum binding energy, b (J/mol) is Temkin isotherm constant and constant B (dimensionless) is related to the heat of adsorption.

Radushkevich [22] and Dubinin [23] have reported that the characteristic sorption curve is related to the porous structure of the sorbent (Table S4). Where the constant, β, ($mmol^2/J^2$) is D-R constant related to the mean free energy of sorption per mole of the sorbate as it is transferred to the surface of the solid from infinite distance in the solution and can be correlated using fallowing relationship

$$E = \frac{1}{\sqrt{2\beta}} \tag{2}$$

and q_m, (mmol/g) is denoted as the single layer capacity. In a deeper explanation, E value indicates the mechanism of the adsorption reaction. When $E < 8\ kJ/mol$, physical forces may affect the adsorption. If E is $8 < E < 16\ kJ/mol$, adsorption is governed by ion exchange mechanism, while for the values of $E > 18\ kJ/mol$, adsorption may be dominated by particle diffusion [7]. The model has often successfully fitted high solute activities and the intermediate range of concentrations data well, but has unsatisfactory asymptotic properties and does not predict the Henry's law at low pressure [7,19]. Meanwhile, the parameter ε known as Polanyi potential and can be correlated as

$$\varepsilon = RT\left(1 + \frac{1}{C_e}\right) \tag{3}$$

where R, T and C_e represent the gas constant (8.314 J/mol K), absolute temperature (K) and adsorbate equilibrium concentration (mg/L), respectively.

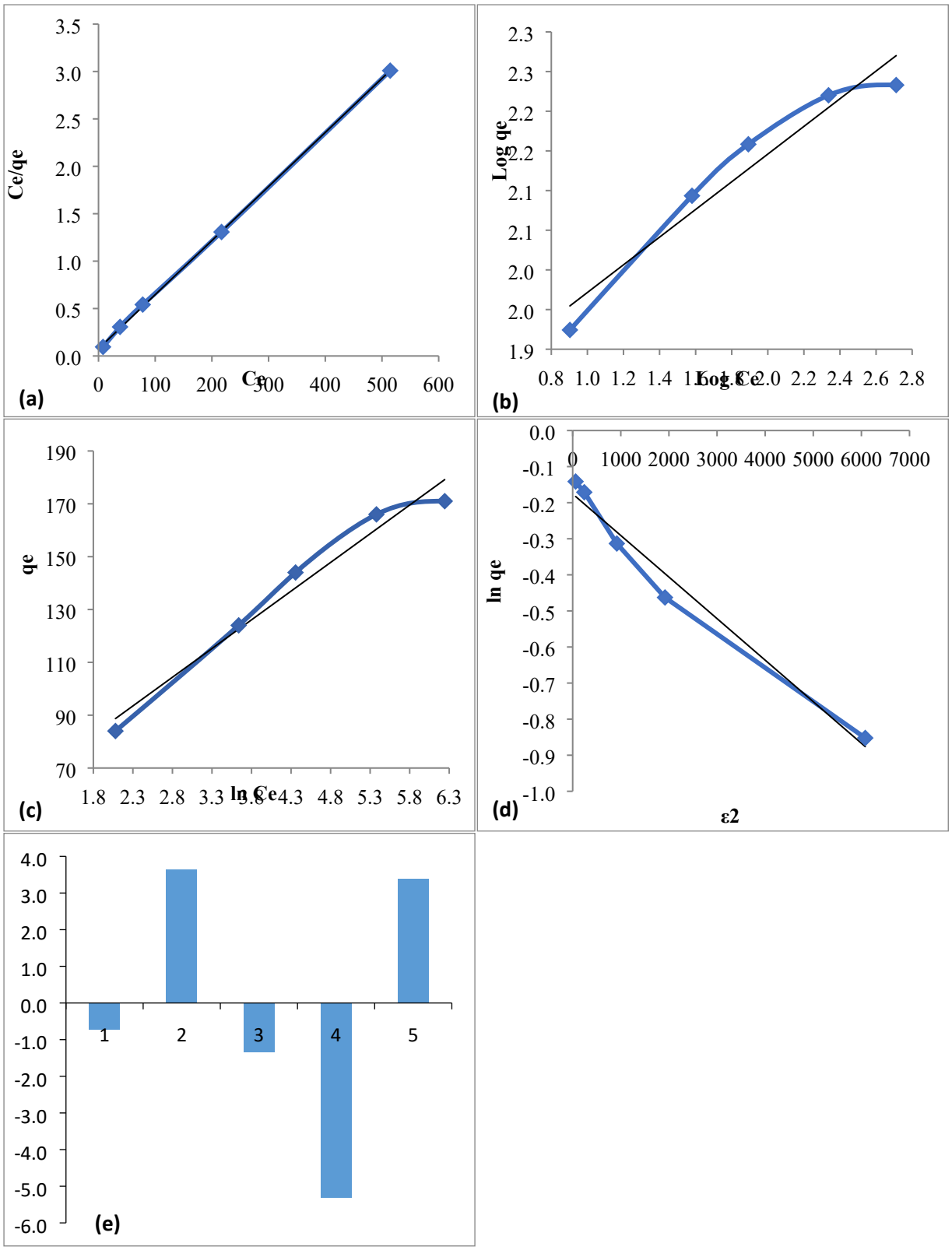

Figure S3. The Langmuir (a), Freundlich (b), Tempkin (c), Dubinin–Radushkevich (d) isotherm regression graphics, parameters and r^2 values and difference between calculated Redlich-Peterson and experimental q_e values for Au (III) adsorption onto APMCM41-Py nanoparticles.

The Redlich-Peterson isotherm contains three parameters ($A(L/g), B(L/mg^{1-1/A}), g$) and incorporates the features of the Langmuir and the Freundlich isotherms [15]. Its equation and linear form can be seen in Table S4. Isotherm unitless constants g is gives between $0 < g < 1$ values. When $g = 1$, adsorption isotherm fits Langmuir isotherm. If $g = 0$, isotherm is now fully Freundlich isotherm [24,25]. Values between this concerned for isotherm representation. Due to having this versatility, it can be applied either in homogeneous or heterogeneous systems.

Figure S3 represents isotherm models linear forms, their linear equation values and correlation coefficients. Also, Figure S3 (e) shows difference between Redlich-Peterson calculated and experimental q_e values for Au (III) adsorption onto APMCM41-Py NPs.

In this study two error functions, the coefficient of determination and nonlinear chi-square test have been used for analyzing the adsorption system. Coefficient of determination is defined as [7]

$$r^2 = \frac{\sum (q_{e,meas} - \bar{q}_{e,calc})^2}{\sum (q_{e,meas} - \bar{q}_{e,calc})^2 + (q_{e,meas} - q_{e,calc})^2} \quad (4)$$

where $q_{e,meas}$ (mg/g) is the amount of dye exchanged by the surface of adsorbent obtained from experiment, $q_{e,calc}$ the amount of adsorbate obtained by isotherm models and $\bar{q}_{e,calc}$ the average of $q_{e,calc}$ (mg/g).

Nonlinear chi-square test is a statistical tool necessary for the best fit of an adsorption system. It is expressed as

$$X^2 = \sum_{i=1}^{n} \frac{(q_{e,calc} - q_{e,meas})^2}{q_{e,meas}} \quad (5)$$

5. Adsorption Thermodynamic

Thermodynamic parameters such as Gibb's free energy (ΔG^0), enthalpy change (ΔH^0) and change in entropy (ΔS^0) for the adsorption of metal ions on APMCM41-Py NPs have been determined by using the following equations

$$\Delta G^0 = \Delta H^0 - T\Delta S^0 \quad (6)$$

$$\Delta G^0 = -RT\ln(K_{ML}) \quad (7)$$

$$\log(K_{ML}) = \frac{\Delta S^0}{2.303\,R} - \frac{\Delta H^0}{2.303\,RT} \quad (8)$$

where q_e is the amount of metal ion adsorbed per unit mass of beads (mg/g), C_e is equilibrium concentration (mg/L) and T is temperature in K and R is the gas constant (8.314 J/molK). K_{LM} is dimensionless Modified Langmuir constant at each temperature. It is calculated from linear regression solve of isotherm equation. Considering the relationship between ΔG^0 and K_L, ΔH^0 and ΔS^0 were determined from the slope and intercept of the van't Hoff plots of $\log(K_{ML})$ versus $1/T$. This pilot can be seen at Figure 6 at the manuscript. Negative values of ΔG^0 confirm the feasibility of the process and the spontaneous nature of the adsorption [7]. The positive value of ΔH^0 is indicating that the adsorption reaction was endothermic. The negative entropy change ($\Delta S°$) for the process was caused by the decrease in degree of freedom of the adsorbed species [21].

REFERENCES

[1] Ignasi Puigdomenech, Hydra and Medusa, R. Inst. Technol. Sweden. (2020) ver. 2020. https://www.kth.se/che/medusa/.

[2] A. Dąbrowski, Adsorption — from theory to practice, Adv. Colloid Interface Sci. 93 (2001) 135–224. https://doi.org/10.1016/S0001-8686(00)00082-8.

[3] S. Lagergren, About the theory of so-called adsorption of soluble substances (org.: Zur theorie der sogenannten adsorption gelöster stoffe), K. Sven. Vetenskapsakademiens Handl. 24 (1898) 1–39.

[4] Y.. Ho, G. McKay, Pseudo-second order model for sorption processes, Process Biochem. 34 (1999) 451–465. https://doi.org/10.1016/S0032-9592(98)00112-5.

[5] Ya. B. Zeldovich, Theoretical foundations of combustion processes, Acta Physicochim. U.R.S.S. 1 (1934) 449–469.

[6] S. Y. Elovich; G. M. Zhabrova, Mechanism of catalytic hydrogenation of ethylene on nickel. 1. Kinetics of the process, Zhur. Fiz. Khim. 13 (1939) 1761–1775.

[7] M. Can, Investigation of the factors affecting acid blue 256 adsorption from aqueous solutions onto red pine sawdust: equilibrium, kinetics, process design, and spectroscopic analysis, Desalin. Water Treat. 57 (2016) 5636–5653. https://doi.org/10.1080/19443994.2014.1003974.

[8] Y. Liu, Y.J. Liu, Biosorption isotherms, kinetics and thermodynamics, Sep. Purif. Technol. 61 (2008) 229–242. https://doi.org/10.1016/j.seppur.2007.10.002.

[9] I. Langmuir, THE ADSORPTION OF GASES ON PLANE SURFACES OF GLASS, MICA AND PLATINUM., J. Am. Chem. Soc. 40 (1918) 1361–1403. https://doi.org/10.1021/ja02242a004.

[10] S. Azizian, S. Eris, L.D. Wilson, Re-evaluation of the century-old Langmuir isotherm for modeling adsorption phenomena in solution, Chem. Phys. 513 (2018) 99–104. https://doi.org/10.1016/j.chemphys.2018.06.022.

[11] H. Freundlich, Über die Adsorption in Lösungen, Zeitschrift Für Phys. Chemie. 57U (1907). https://doi.org/10.1515/zpch-1907-5723.

[12] V.P. M.I. Temkin, “Kinetics of ammonia synthesis on promoted iron catalyst,” Acta USSR. 12 (1940) 327–356.

[13] M.M. Dubinin, The Potential Theory of Adsorption of Gases and Vapors for Adsorbents with Energetically Nonuniform Surfaces., Chem. Rev. 60 (1960) 235–241. https://doi.org/10.1021/cr60204a006.

[14] M.M. Dubinin, Fundamentals of the theory of adsorption in micropores of carbon adsorbents: Characteristics of their adsorption properties and microporous structures, Carbon N. Y. 27 (1989) 457–467. https://doi.org/10.1016/0008-6223(89)90078-X.

[15] O. Redlich, D.L. Peterson, A Useful Adsorption Isotherm, J. Phys. Chem. 63 (1959) 1024–1024. https://doi.org/10.1021/j150576a611.

[16] I. Langmuir, The constitution and fundamental properties of solids and liquids. Part I. Solids, J. Am. Chem. Soc. (1916). https://doi.org/10.1021/ja02268a002.

[17] B.H.J. Hofstee, Non-inverted versus inverted plots in enzyme kinetics, Nature. (1959). https://doi.org/10.1038/1841296b0.

[18] G. Scatchard, The Attractions of Proteins for Small Molecules and Ions, Ann. N. Y. Acad. Sci. 51 (1949) 660–672. https://doi.org/10.1111/j.1749-6632.1949.tb27297.x.

[19] K.Y. Foo, B.H. Hameed, Insights into the modeling of adsorption isotherm systems, Chem. Eng. J. 156 (2010) 2–10. https://doi.org/10.1016/j.cej.2009.09.013.

[20] T.W. Weber, R.K. Chakravorti, Pore and solid diffusion models for fixed-bed adsorbers, AIChE J. 20 (1974) 228–238. https://doi.org/10.1002/aic.690200204.

[21] M. Can, Equilibrium, kinetics and process design of acid yellow 132 adsorption onto red pine sawdust, Water Sci. Technol. 71 (2015) 1901–1911. https://doi.org/10.2166/wst.2015.164.

[22] L. V. Radushkevich, Potential theory of sorption and structure of carbons, Zhurnal Fiz. Khimii. 23 (1949) 1410–1420.

[23] M.M. Dubinin, Adsorption in micropores, J. Colloid Interface Sci. 23 (1967) 487–499. https://doi.org/10.1016/0021-9797(67)90195-6.

[24] K.V. Kumar, S. Sivanesan, Comparison of linear and non-linear method in estimating the sorption isotherm parameters for safranin onto activated carbon, J. Hazard. Mater. 123 (2005) 288–292. https://doi.org/10.1016/j.jhazmat.2005.03.040.

[25] M. Sayın, M. Can, M. İmamoğlu, M. Arslan, 1,3,5-Triazine-pentaethylenehexamine polymer for the adsorption of palladium (II) from chloride-containing solutions, React. Funct. Polym. 88 (2015) 31–38. https://doi.org/10.1016/j.reactfunctpolym.2015.02.003.